

Design, synthesis, and evaluation of potential inhibitors of nitric oxide synthase

Tania Castaño, Arantxa Encinas, Concepción Pérez, Ana Castro,[†]
Nuria E. Campillo* and Carmen Gil*

Instituto de Química Médica, (CSIC), Juan de la Cierva 3, 28006 Madrid, Spain

Received 29 January 2008; revised 8 April 2008; accepted 16 April 2008

Available online 18 April 2008

Abstract—Selective inhibitors of neuronal nitric oxide synthase (nNOS) were shown to protect brain and may be useful in the treatment of neurodegenerative diseases. In this context, our purpose has been to design and synthesize a new family of derivatives of thiadiazoles as possible inhibitors of nNOS. To achieve it a supervised artificial neural network model has been developed for the prediction of inhibition of Nitric Oxide Synthase using a dataset of 119 nNOS inhibitors. The definition of the molecules was achieved from a not-supervised neural network using a home made program named CODES. Also, thiadiazole-based heterocycles, previously predicted, were prepared as conformationally restricted analogues of a selective nNOS inhibitor, *S*-ethyl *N*-phenylisothiurea.

© 2008 Elsevier Ltd. All rights reserved.

1. Introduction

Neuroprotection is one of the major challenges of modern medicine for the treatment of chronic, progressive and neurodegenerative disorders such as Alzheimer's disease, Parkinson's disease, and multiple sclerosis. The protection of neurons and their synapses against damage and death, and the preservation of their functions could provide effective cure for these pathologies.^{1–3}

The brain is particularly vulnerable to oxidative damage because of the high rate of oxygen utilization, the high content of oxidizable polyunsaturated fatty acids, and of redox-active transition metal ions that can generate free radicals. Moreover, the relative dearth of antioxidant protective defenses renders the central nervous system (CNS) particularly prone to oxidative damage.⁴ It is widely accepted that oxidative stress increases during aging and recent evidences suggest its important role

in the origin and in the development of neurodegenerative diseases such as Alzheimer's disease (AD).⁵ The fact that the oxidative damage found in some biomolecules is an event that precedes the characteristic lesions of AD namely, senile plaques and neurofibrillary tangles, supports the idea that oxidative stress is an early event in neurodegeneration.^{6,7} Thus, drugs that directly scavenge free radicals or inhibit enzymes implicated in their production could be therapeutically useful in AD.⁸ One of these enzymes is nitric oxide synthase (NOS) which produces nitric oxide (NO). Excessive production of NO by activated glial cells contributes to inflammation-related neurodegenerative processes. In fact, expression and activity of NOS play an important role in the maintenance and increase of NO liberation in neurons which makes it an attractive therapeutic objective in the search of neuronal protective agents.⁹

There are three isoenzymes of NOS which include a neuronal enzyme (nNOS), an endothelial enzyme (eNOS), and an inducible enzyme (iNOS). Although these three enzymes have cofactor requirements in common and similar mechanism of action, they are structurally distinct from one another.¹⁰ The research and clinical utility of NOS inhibitors are dependent on both their specificity and their potency of inhibition. Selective NOS isoform inhibition to regulate NO synthesis has received much attention. Inhibitors with high isoform

Keywords: NOS; Artificial neural network; CODES; QSAR; Thiadiazole.

* Corresponding authors. Tel.: +34 915622900; fax: +34 915644853 (NEC; CG); e-mail addresses: nuria@suricata.iqm.csic.es; cgil@iqm.csic.es

[†] Present address: NeuroPharma, S.A., Avda. de la Industria 52, 28760 Tres Cantos, Madrid, Spain.

selectivity are required to further define the role of each NOS isoform in various biological processes.¹¹ The majority of described inhibitors to date are analogues of the endogenous substrate L-arginine.¹²

Due to the fact that nNOS is the primary NO regulator in neurons, selective inhibitors of this isoenzyme were shown to protect brain and may be useful in the treatment of neurodegenerative diseases.^{13,14} The aim of this article is the study of new-design compounds based on thiadiazole framework, conformationally restricted analogues of a selective nNOS inhibitor *S*-ethyl *N*-phenylthiostiourea, as possible nNOS inhibitors. To achieve this goal we developed a neural network model based on known nNOS inhibitor to predict their activity. The synthesis and evaluation of nNOS inhibitors of thiadiazole derivatives with aryl substituents are also presented here.

2. Results and discussions

2.1. Neural network model

The quantitative structure–activity relationship was performed by means of artificial neural network system using NOS inhibitor families previously described (Table 1). This family is formed by isothiouras,^{15–17} bisisothiouras,^{15–17} arylisothiouras,¹⁸ aminoguanidines,^{19,20} nitroguanidines,^{21–24} arylamidines,²⁵ ornitine derivatives,²⁶ thiazole and thiazoline,¹⁷ imidazole,^{23,27–29} and pyrazole³⁰ (see Fig. 1).

As a theoretical tool, the Artificial Neural Networks (ANNs) are a modeling methodology whose application in some areas of Medicinal Chemistry such as quantitative structure–property relationship (QSPR), quantitative structure–activity relationship (QSAR) and prediction of pharmacokinetic properties has increased spectacularly in recent years.^{31–35}

The development of nonlinear modeling approaches, such as artificial intelligence-based algorithms, opened up the field to the concurrent analysis of a wider variety of structures with potentially varying modes of action and noncongeneric chemicals. These artificial systems emulate the function of the brain, where a very high number of information-processing neurons are interconnected and are known for their ability to model a wide set of functions, including linear and nonlinear, without knowing the analytic forms in advance.

To overcome the first step, we used an original homemade program called CODES[®].³⁶ CODES is an efficient and easy-to-use program to encode chemical structures by means of neural computing. The molecular descriptors obtained from this method contain all the underlying information of their chemical structure. The original CODES program was created and developed by Prof. Manfred Stud in Instituto de Química Médica (IQM, Madrid, Spain). At present, CODES program continues being further developed and optimized by our research group in collaboration with Advanced Software Produc-

tion Line S.L. CODES program is available at <http://www.iqm.csic.es>.

This singular way to encode chemical entities converts CODES into an excellent tool to carry out QSAR and QSPR studies.^{37–40} Thus, the numeric descriptors generated by CODES have been used as input data in feed-forward back-propagation network to obtain a predict model (see Section 4).

Using the strategy gathered in Figure 2, we have developed different neural network models for the prediction of nNOS inhibition.

The first step in this procedure is the codification of the whole dataset using CODES program, to define the molecules from a topological point of view. CODES generates for each molecule a dynamic matrix ($A \times R$), where A is the number of atoms of each structure and R is the number of iterations necessary to achieve convergence in the codification process. In order to have the same number of descriptors for each structure we developed two different strategies (see Section 4). One of these two strategies is using the whole matrix of each compound and following of the data reduction process to obtain the same descriptor number for each chemical structure without losing any structural data (strategy 1). The other strategy is used to choose the parameters from the last step of the codification process generated by CODES. We decided to employ the descriptors of the four atoms more conserved in all the structures (Fig. 3) (see supporting information, Tables S1 and S2).

It is well-known that the quality of QSAR models is affected by the dataset partition. Thus, the original database was randomly divided into two sets, the training set and the test set. Furthermore, to account for sampling error, models were generated from different training/test set partitions. Thus, the training set of different sizes (50–80 compounds) was generated randomly. Regarding the architecture of the models, specially the number of neurons in hidden layer was optimized in each network. Unfortunately, the models developed with quantitative data using both the strategies were not statistically acceptable. The results in the training process using strategy 1 were r values between 0.78 and 0.98, r_{cv}^2 values between 0.57 and 0.95, and the s values between 0.17 and 0.58. However, the prediction ability of the models was poor in the external validation process. Regarding strategy 2, the results were analogous ($s = 0.33–0.46$, $r = 0.77–0.91$, and $r_{cv}^2 = 0.59–0.80$).

To overcome these results, we re-addressed the problem from a qualitative point of view. Thus, the compounds were clustered into three groups, active (1), moderate (0), or inactive (–1) (Section 4). The statistical results together with the results of the internal validation are gathered in Table 2 for different training sets and both the strategies.

At the first glance, these results indicate that the best models are model 2 (strategy 1) and model 6 (strategy 2), which show the highest values of r and r_{cv}^2 and

Table 1. K_i values of nNOS dataset

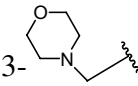
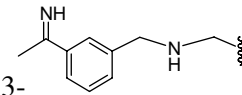
| Inhibitor (I) | R | nNOS (K_i , μM) | Lit. |
|---------------|---|-----------------------------------|-------|
| I-1 | CH ₃ | 0.16 | 15–17 |
| I-2 | CH ₂ CH ₃ | 0.029 | 15–17 |
| I-3 | CH(CH ₃) ₂ | 0.037 | 15–17 |
| I-4 | C(CH ₃) ₃ | 0.62 | 15–17 |
| I-5 | CH ₂ CH ₂ CH ₃ | 0.63 | 15–17 |
| I-6 | CH ₂ Ph | 14 | 15–17 |
| I-7 | CH ₂ CH ₂ Ph | 0.80 | 15–17 |
| I-8 | CH ₂ CH ₂ CH ₂ Ph | 14 | 15–17 |
| I-9 | CH ₂ CH ₂ NH ₂ | 1.80 | 15–17 |
| I-10 | CH ₂ CH=C(CH ₃) ₂ | 2.00 | 15–17 |
| I-11 | -(CH ₂) ₂ -(1,3-Ph)-(CH ₂) ₂ - | 0.25 | 15–17 |
| I-12 | -(CH ₂) ₂ -(1,4-Ph)-(CH ₂) ₂ - | 0.016 | 15–17 |
| I-13 | -(CH ₂) ₂ -(1,4-Ph)-(CH ₂)- | 0.1 | 15–17 |
| I-14 | -(CH ₂) ₃ -(1,3-Ph)-(CH ₂) ₃ - | 4.8 | 15–17 |
| I-15 | H | 0.12 | 18 |
| I-16 | 2-Br | 0.25 | 18 |
| I-17 | 2-Cl | 0.17 | 18 |
| I-18 | 3-Cl | 0.45 | 18 |
| I-19 | 4-Cl | 0.14 | 18 |
| I-20 | 2-OCH ₃ | 0.17 | 18 |
| I-21 | 3-OCH ₃ | 0.56 | 18 |
| I-22 | 4-OCH ₃ | 0.29 | 18 |
| I-23 | 4-OCF ₃ | 0.70 | 18 |
| I-24 | 4-OPh | 0.19 | 18 |
| I-25 | 4-OCH ₂ Ph | 0.21 | 18 |
| I-26 | 4-OH | 0.34 | 18 |
| I-27 | 4-COOEt | 1.6 | 18 |
| I-28 | 3-COOH | 11 | 18 |
| I-29 | 4-CH ₃ | 0.18 | 18 |
| I-30 | 2-iPr | 1.1 | 18 |
| I-31 | 4-iPr | 0.33 | 18 |
| I-32 | 4-c-C ₆ H ₁₁ | 1.5 | 18 |
| I-33 | 2-CF ₃ | 1.4 | 18 |
| I-34 | 3-CF ₃ | 1.1 | 18 |
| I-35 | 4-CF ₃ | 0.32 | 18 |
| I-36 | 4-NO ₂ | 0.66 | 18 |
| I-37 | 4-N(CH ₃) ₂ | 1.4 | 18 |
| I-38 | Ar = 2-pyridil | 4.8 | 18 |
| I-39 | Ar = 3-pyridil | 1.0 | 18 |
| I-40 | Ar = 4-pyridil | 0.8 | 18 |
| I-41 | H | 3.3 | 19,20 |
| I-42 | CH ₃ | 14 | 19,20 |
| I-43 | CH ₂ CH ₃ | 1.0 | 19,20 |
| I-44 | OH | 0.68 | 19,20 |
| I-45 | Ph | 4.0 | 19,20 |
| I-46 | — | 0.10 | 21–24 |
| I-47 | — | 1.1 | 21–24 |
| I-48 | — | 0.13 | 21–24 |
| I-49 | — | 0.5 | 21–24 |
| I-50 | 3-CH ₂ NH ₂ | 0.04 | 25 |
| I-51 | 4-CH ₂ NH ₂ | 1.5 | 25 |
| I-52 | 3-NH ₂ | 14 | 25 |
| I-53 | 3-CH ₂ CH ₂ NH ₂ | 1 | 25 |
| I-54 | 3-CH ₂ NHMe | 0.056 | 25 |
| I-55 | 3-CH ₂ NMe ₂ | 0.17 | 25 |
| I-56 |  | 2.8 | 25 |
| I-57 | 3-CH ₂ NHOH | 2.1 | 25 |
| I-58 | 3-CH ₂ NHC(NH)Me | 0.37 | 25 |
| I-59 |  | 0.042 | 25 |

Table 1 (continued)

| Inhibitor (I) | R | nNOS (K_i , μM) | Lit. |
|---------------|---|-----------------------------------|-------|
| I-60 | 3-CH ₂ SC(NH)NH ₂ | 0.36 | 25 |
| I-61 | 3-SO ₂ NH ₂ | 29 | 25 |
| I-62 | 3-NHNH ₂ | 1.1 | 25 |
| I-63 | 3-C(NH)NH ₂ | 0.57 | 25 |
| I-64 | 3-NHC(NH)Me | 1.5 | 25 |
| I-65 | R ₁ = CH ₂ NH ₂ , R ₂ = Me | 0.04 | 25 |
| I-66 | R ₁ = CH ₂ NH ₂ , R ₂ = CH ₂ NH ₂ | 0.19 | 25 |
| I-67 | R ₁ = CH ₂ NH ₂ , R ₂ = CH ₂ SMe | 0.011 | 25 |
| I-68 | R ₁ = CH ₂ NH ₂ , R ₂ = CH ₂ F | 0.011 | 25 |
| I-69 | R ₁ = CH ₂ OH, R ₂ = CH ₂ F | 0.30 | 25 |
| I-70 | R ₁ = CH ₂ NH ₂ , R ₂ = 2-pyridiyl | 0.33 | 25 |
| I-71 | R ₁ = CH ₂ NH ₂ , R ₂ = 2-furanyl | 0.0063 | 25 |
| I-72 | R ₁ = CH ₂ NH ₂ , R ₂ = 2-thienyl | 0.0087 | 25 |
| I-73 | H | 1.7 | 26 |
| I-74 | -CH=CH ₂ | 0.1 | 26 |
| I-75 | Me | 3 | 26 |
| I-76 | -CH ₂ CH ₃ | 5.3 | 26 |
| I-77 | R ₁ , R ₂ = H | 12 | 17 |
| I-78 | R ₁ = Me, R ₂ = H | 10 | 17 |
| I-79 | R ₁ = H, R ₂ = Me | 1.1 | 17 |
| I-80 | R ₁ , R ₂ = Me | 0.38 | 17 |
| I-81 | R ₁ = -CH ₂ CH ₂ Ph, R ₂ = H | 0.89 | 17 |
| I-82 | — | 0.41 | 17 |
| I-83 | n = 3, R = 4-Br | 125 | 23 |
| I-84 | n = 4, R = 4-Br | 32 | 23 |
| I-85 | n = 6, R = 4-Br | 57 | 23 |
| I-86 | n = 3, R = 4-CF ₃ | 75 | 23 |
| I-87 | n = 4, R = 4-CF ₃ | 94 | 23 |
| I-88 | n = 6, R = 4-CF ₃ | 35 | 23 |
| I-89 | n = 4, R = 2-Br | 180 | 23 |
| I-90 | n = 4, R = 3-Br | 60 | 23 |
| I-91 | n = 2, R = 4-Br | 125 | 23 |
| I-92 | n = 2, R = 4-CF ₃ | 45 | 23 |
| I-93 | n = 0, R = H | 170 | 27 |
| I-94 | n = 1, R = H | 2 | 27 |
| I-95 | n = 2, R = H | 65 | 27 |
| I-96 | n = 3, R = H | 2 | 27 |
| I-97 | n = 4, R = H | 150 | 27 |
| I-98 | n = 1, R = Ph | 80 | 27 |
| I-99 | n = 2, R = Ph | 100 | 27 |
| I-100 | n = 3, R = Ph | 70 | 27 |
| I-101 | — | 74 | 28,29 |
| I-102 | — | 105 | 28,29 |
| I-103 | — | 375 | 28,29 |
| I-104 | — | 175 | 28,29 |
| I-105 | — | 125 | 28,29 |
| I-106 | — | 175 | 28,29 |
| I-107 | — | 430 | 28,29 |
| I-108 | H | 0.4 | 30 |
| I-109 | Propyl | 3 | 30 |
| I-110 | Butyl | 14 | 30 |
| I-111 | Pentyl | 60 | 30 |
| I-112 | Cyclopropyl | 50 | 30 |
| I-113 | Cyclopropylmethyl | 10 | 30 |
| I-114 | Isobutyl | 45 | 30 |
| I-115 | R ₁ = CH ₃ , R ₂ = H, R ₃ = H | 8 | 30 |
| I-116 | R ₁ = H, R ₂ = CH ₃ , R ₃ = H | 12 | 30 |
| I-117 | R ₁ = CH ₃ , R ₂ = H, R ₃ = CH ₃ | 350 | 30 |
| I-118 | — | 6 | 30 |
| I-119 | — | 2 | 30 |

regarding internal validation, in both cases, the prediction is 100% (4/4). However, according to the statistical indexes (Table 3), the models obtained with strategy 1

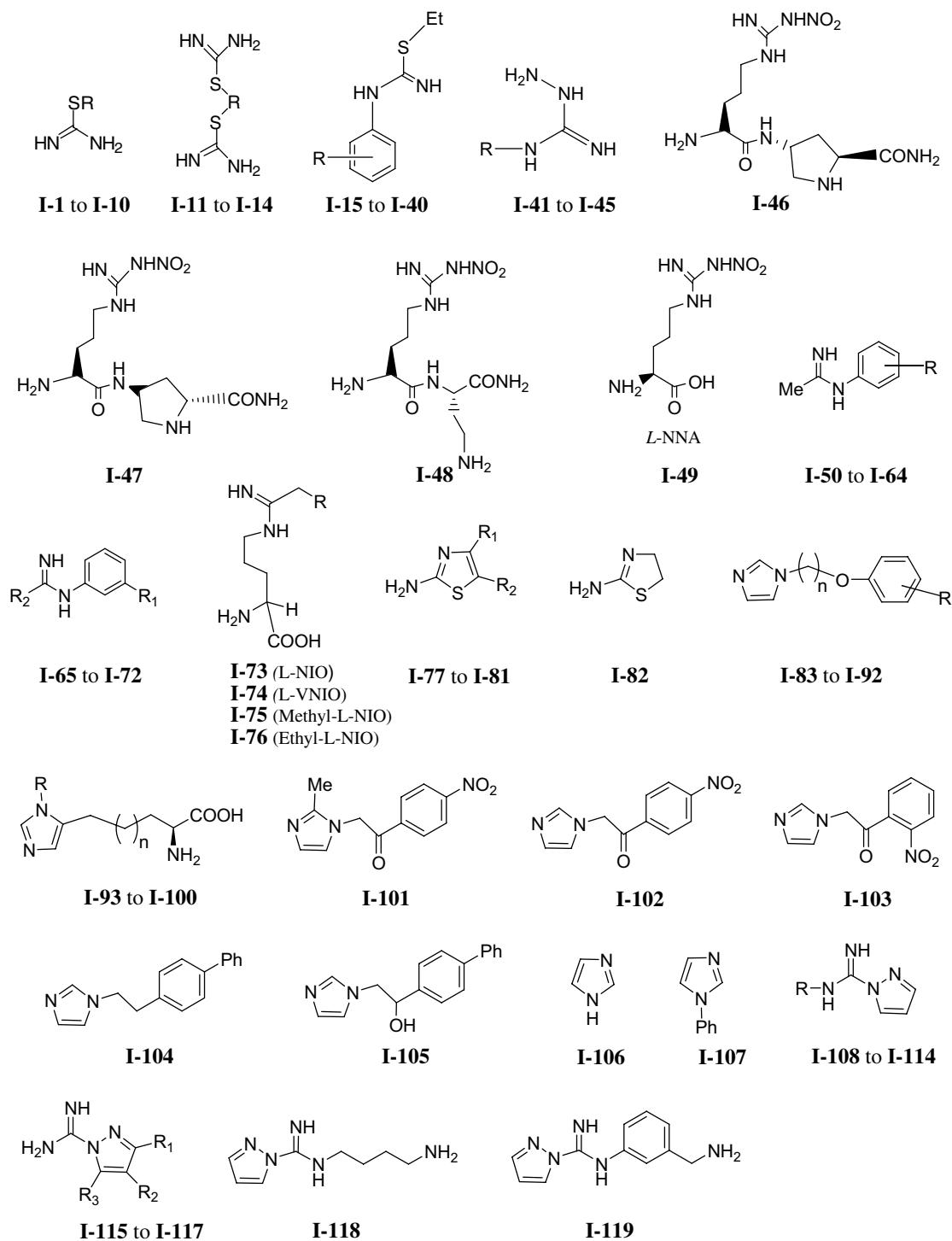


Figure 1. NOS inhibitor families.

(models 1, 2, 3, and 4) show lower values of index fraction correct (FC) the probability of detection (POD) and higher values of false alarm rate (FAR) than the models obtained with strategy 2 (models 5, 6, and 7) pointing out that there is a high percentage of misclassified inactive compounds (classified as active compounds) and therefore, these models seem not to detect real inhibitors (see Section 4).

The models obtained using the strategy 2 show better values of FC, FAR, and POD, with the model 7, the best

one, showing the highest values of FC and POD and the lowest value of FAR.

From these results, the best net is model 7, which uses the static vector as definition of the structures (strategy 2). The model shows a good overall classification percentage of 91 in the training set. A total of 89% of the compounds in the external prediction set were correctly identified by the model. The results of the training and test sets are gathered in Tables 4 and 5, respectively.

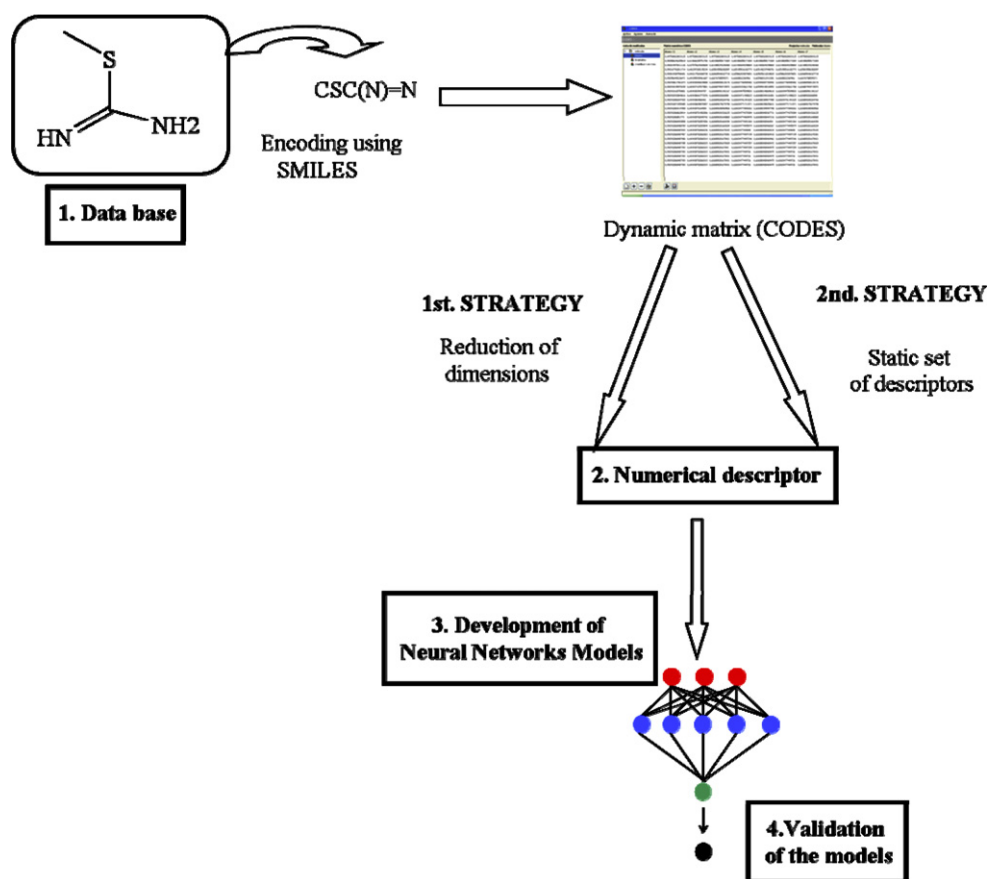


Figure 2. General methodology to develop an inhibition NOS model.

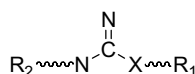


Figure 3. Atom template to static set descriptor.

The percentages of correct classifications for the three categories in the training set and test set are shown in Figures 4 and 5. Analysis of the classification by category shows that the model correctly evaluates 100% for active compounds (1), 33% for moderates and 91% for inactive (−1) in training sets and 92% for active compounds (1), 50% for moderates and 100% for inactives (−1) in test sets.

Table 3. Test statistical indices

| Models | FC (%) | FAR (%) | POD (%) |
|--------|--------|---------|---------|
| 1 | 43.33 | 84.61 | 72.72 |
| 2 | 43.33 | 92.30 | 66.66 |
| 3 | 62.06 | 33.33 | 72.22 |
| 4 | 62.06 | 27.77 | 75.00 |
| 5 | 70.58 | 25.00 | 81.81 |
| 6 | 76.47 | 15.38 | 81.81 |
| 7 | 89.47 | 5.88 | 92.85 |
| 8 | 72.00 | 22.22 | 78.57 |

Once the neural model was developed, we used it to predict the activity of new design compounds. Griffith⁴¹ and Furfine¹⁸ have reported that L-thiocitrulline (**1**) and S-ethyl N-phenylisothiourea (**2**) are potent NOS inhibitors with selectivity for the neuronal isoform.

Table 2. nNOS model statistical parameters

| Models | Strategy | Architecture | n_{training} | s | r | r_{cv}^2 | Internal validation ^a |
|--------|----------|--------------|-----------------------|------|------|-------------------|----------------------------------|
| 1 | 1 | 4:7:1 | 77 | 0.22 | 0.96 | 0.92 | 3/4 |
| 2 | 1 | 4:7:1 | 68 | 0.08 | 0.99 | 0.98 | 4/4 |
| 3 | 1 | 4:7:1 | 69 | 0.25 | 0.95 | 0.91 | 3/4 |
| 4 | 1 | 4:7:1 | 71 | 0.37 | 0.90 | 0.80 | 3/4 |
| 5 | 2 | 4:5:1 | 59 | 0.26 | 0.93 | 0.87 | 4/4 |
| 6 | 2 | 4:5:1 | 57 | 0.20 | 0.96 | 0.92 | 4/4 |
| 7 | 2 | 4:5:1 | 55 | 0.36 | 0.89 | 0.78 | 4/4 |
| 8 | 2 | 4:7:1 | 68 | 0.36 | 0.89 | 0.79 | 3/4 |

^a Correct prediction of the randomly excluded data.

Table 4. Training set of model 7

| Compound | K_i (μM) | Group ^a | Predicted group |
|----------|-------------------------|--------------------|-----------------|
| I-3 | 0.037 | 1 | 1 |
| I-4 | 0.62 | 1 | 1 |
| I-5 | 0.63 | 1 | 1 |
| I-6 | 14 | -1 | -1 |
| I-7 | 0.8 | 1 | 1 |
| I-8 | 14 | -1 | 1 |
| I-10 | 2 | 0 | 0 |
| I-11 | 0.25 | 1 | 1 |
| I-12 | 0.016 | 1 | 1 |
| I-13 | 0.1 | 1 | 1 |
| I-15 | 0.12 | 1 | 1 |
| I-16 | 0.25 | 1 | 1 |
| I-18 | 0.45 | 1 | 1 |
| I-20 | 0.17 | 1 | 1 |
| I-21 | 0.56 | 1 | 1 |
| I-22 | 0.29 | 1 | 1 |
| I-23 | 0.7 | 1 | 1 |
| I-24 | 0.19 | 1 | 1 |
| I-26 | 0.34 | 1 | 1 |
| I-29 | 0.18 | 1 | 1 |
| I-31 | 0.33 | 1 | 1 |
| I-35 | 0.32 | 1 | 1 |
| I-36 | 0.66 | 1 | 1 |
| I-40 | 0.8 | 1 | 1 |
| I-41 | 3.3 | 0 | 1 |
| I-49 | 0.5 | 1 | 1 |
| I-50 | 0.04 | 1 | 1 |
| I-51 | 1.5 | 0 | 1 |
| I-53 | 1 | 1 | 1 |
| I-55 | 0.17 | 1 | 1 |
| I-58 | 0.37 | 1 | 1 |
| I-59 | 0.042 | 1 | 1 |
| I-60 | 0.36 | 1 | 1 |
| I-62 | 1.1 | 0 | 1 |
| I-63 | 0.57 | 1 | 1 |
| I-65 | 0.04 | 1 | 1 |
| I-66 | 0.19 | 1 | 1 |
| I-67 | 0.011 | 1 | 1 |
| I-68 | 0.011 | 1 | 1 |
| I-69 | 0.3 | 1 | 1 |
| I-72 | 0.0087 | 1 | 1 |
| I-74 | 0.1 | 1 | 1 |
| I-77 | 12 | -1 | -1 |
| I-78 | 10 | -1 | -1 |
| I-81 | 0.89 | 1 | 1 |
| I-101 | 74 | -1 | -1 |
| I-108 | 0.4 | 1 | 1 |
| I-109 | 3 | 0 | -1 |
| I-110 | 14 | -1 | -1 |
| I-111 | 60 | -1 | -1 |
| I-114 | 45 | -1 | -1 |
| I-116 | 12 | -1 | -1 |
| I-117 | 350 | -1 | -1 |
| I-118 | 6 | -1 | -1 |
| I-119 | 2 | 0 | 0 |

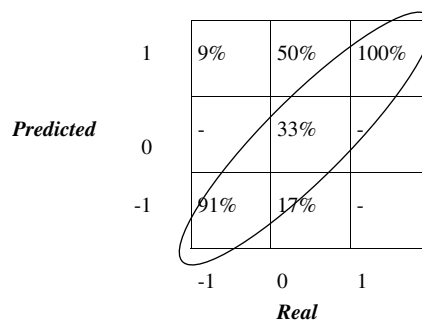
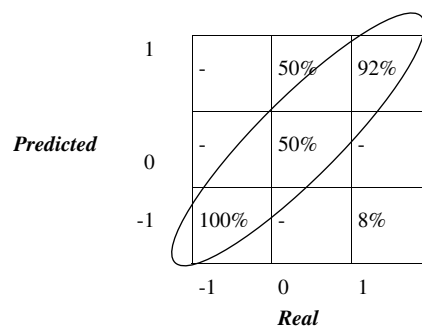
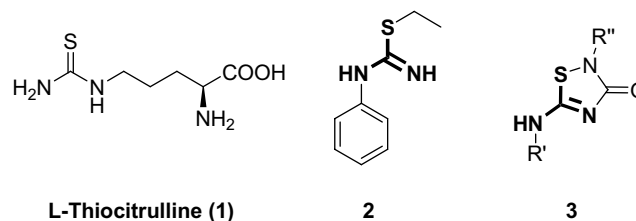
^a Active (1), moderate (0) or inactive (-1).

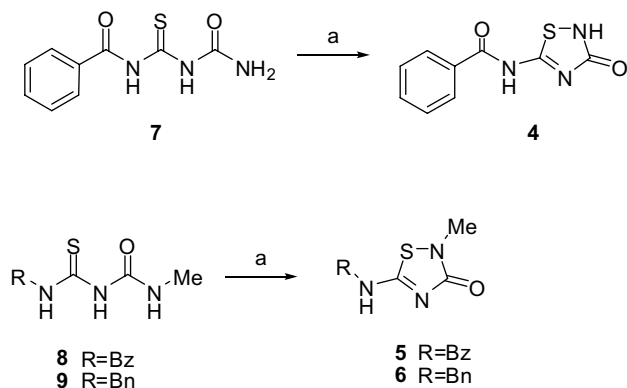
Taking into account these results we proposed the synthesis of thiadiazole derivatives with aryl substituents (3), which can be considered as conformationally restricted analogues of *S*-ethyl *N*-phenylisothiourea (2) (Fig. 6). This scaffold should not only be able to donate hydrogen bonds (assuming that the ring nitrogen remains protonated at physiological pH), but also make non-polar contacts. These two interactions have been

Table 5. Test set of model 7

| Compound | K_i (μM) | Group ^a | Predicted group |
|----------|-------------------------|--------------------|-----------------|
| I-1 | 0.16 | 1 | 1 |
| I-2 | 0.029 | 1 | 1 |
| I-17 | 0.17 | 1 | 1 |
| I-19 | 0.14 | 1 | 1 |
| I-25 | 0.21 | 1 | 1 |
| I-39 | 1 | 1 | 1 |
| I-43 | 1 | 1 | 1 |
| I-46 | 0.1 | 1 | 1 |
| I-47 | 1.1 | 0 | 1 |
| I-48 | 0.13 | 1 | 1 |
| I-52 | 14 | -1 | -1 |
| I-54 | 0.056 | 1 | 1 |
| I-56 | 2.8 | 0 | 0 |
| I-70 | 0.33 | 1 | 1 |
| I-71 | 0.0063 | 1 | 1 |
| I-80 | 0.38 | 1 | -1 |
| I-112 | 50 | -1 | -1 |
| I-113 | 10 | -1 | -1 |
| I-115 | 8 | -1 | -1 |

^a Active (1), moderate (0) or inactive (-1).

**Figure 4.** Analysis of the classification by category in training set of model 7.**Figure 5.** Analysis of the classification by category in test set of model 7.**Figure 6.** Structure of *S*-ethyl *N*-phenylisothiourea.



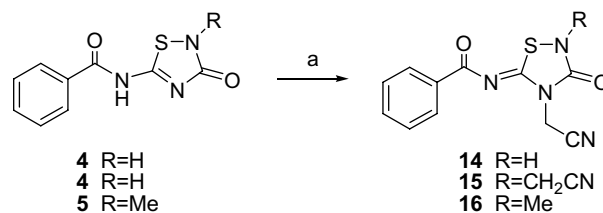
Scheme 1. Reagents and condition: (a) NBS, MeOH, reflux, 12 h (compound **4**: 76%, **5**: 86%, **6**: 80%).

shown as important requirements for the NOS inhibitory activity of isothioureas.⁴² Departing from the framework **2** (Fig. 6) we proposed several aminothiadiazoles in order to predict their activity as nNOS inhibitors. All the considered compounds were predicted as active except when the amino at position 5 is not substituted, pointing out that it is necessary for the activity that the amino in this position will be substituted. In addition, these initial structures could be functionalized subsequently in order to obtain an extensive family of compounds.

2.2. Synthesis and NOS evaluation

The 5-amino-1,2,4-thiadiazole-3-ones **4**, **5**, and **6** described as GSK-3 β inhibitors⁴³ were obtained by oxidative cyclization of thiobiurets **7**, **8**, and **9** via N–S bond formation with *N*-bromosuccinimide⁴⁴ (Scheme 1). Previously, the thiobiurets **7**, **8** and **9** were prepared by condensation of isothiocyanates with urea⁴⁵ or methylurea.⁴⁶

The diversification of 5-benzylamino-2-methyl-3-oxo-2,3-dihydro-1,2,4-thiadiazole (**6**) by addition of isocyanates and isothiocyanates in the presence of triethylamine yielded the imino derivatives, **10–13**, the structures of which were elucidated on the basis of NMR experiments. These thiadiazoles were obtained after an addition–rearrangement reaction,⁴⁷ and the presence of an amide group should allow the molecule to establish

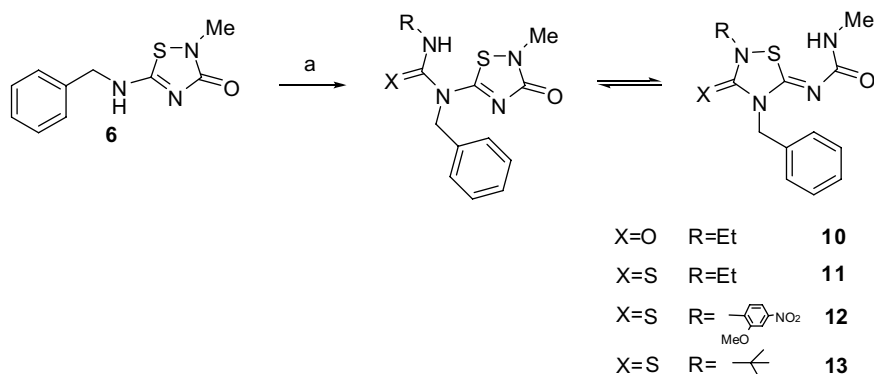


Scheme 3. Reagents and condition: (a) ClCH₂CN, K₂CO₃, DMF, 60–80 °C, 2.5–22 h (compound **14**: 60%, **15**: 75%, **16**: 97%).

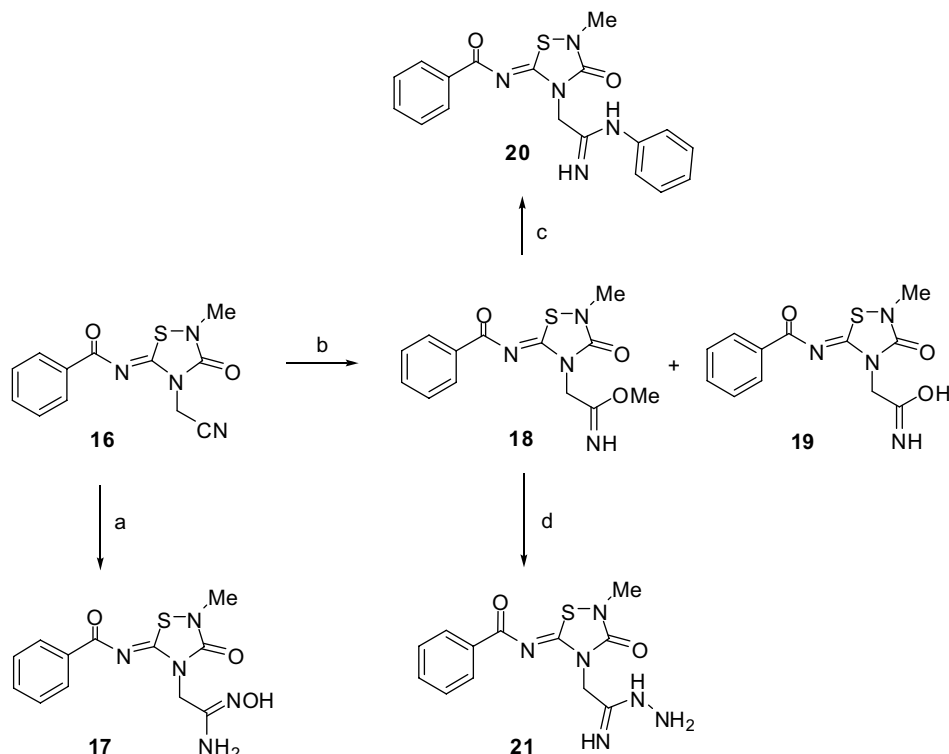
hydrogen bonds in the NOS active site (Scheme 2). Benzoylamino derivatives **4** and **5** did not react in these conditions due to the coordination between the hypervalent sulfur and the carbonyl group, which has been postulated in similar heterocycles,⁴⁸ and that would imply the blockade of the atom of sulfur for the addition reaction.

In order to introduce a cyano functionality in the heterocycles, the alkylation of compounds **4** and **5** with chloroacetonitrile was performed following the described procedures for related compounds.⁴⁵ The best results were achieved by using potassium carbonate as a base in anhydrous dimethylformamide followed by condensation with chloroacetonitrile. Starting from 5-benzoylamino-3-oxo-2,3-dihydro-1,2,4-thiadiazole (**4**), a mixture of mono- and dialkylated derivatives (**14** and **15**, respectively) was obtained. Obviously, when the starting material was 5-benzoylamino-2-methyl-3-oxo-2,3-dihydro-1,2,4-thiadiazole (**5**), only the monoalkylated product **16** was formed (Scheme 3).

Taking into account that amidine group appears to be a common pharmacophore of NOS inhibitors,¹² we took advantage of the nitrile group reactivity present in the thiadiazol framework to prepare different related analogues as amidoxime **17**, imido ester **18**, or amidines **20** and **21** from 5-benzoylimino-4-cyanomethyl-2-methyl-3-oxo-2,3,4,5-tetrahydro-1,2,4-thiadiazole (**16**). In order to generate amidoxime **17**, hydroxylamine was added to the cyano group of **16** according to a previously described procedure.⁴⁹ On the other hand, compound **16** was transformed into the imido ester **18** by the Pinner synthesis,^{50,51} where also traces of the hydrolysis by-product **19** were also identified. Finally, amidine



Scheme 2. Reagents and condition: (a) RNCX, Et₃N, DMF, 80 °C, 5–48 h (compound **10**: 79%, **11**: 46%, **12**: 26%, **13**: 20%).



Scheme 4. Reagents and conditions: (a) Et_3N , $\text{NH}_2\text{OH}\cdot\text{HCl}$, DMSO, 75 °C, 8 h (85%); (b) NaOMe/MeOH , rt, 4 h (**18**: 92%); (c) NH_2Ph , 40 °C, 32 h (6%); (d) $\text{NH}_2\text{NH}_2\cdot\text{HCl}$, 45 °C, 72 h (48%).

derivatives **20** and **21** were obtained by reaction with aniline and hydrazine, respectively⁵¹ (Scheme 4), but unfortunately they decomposed after their characterization.

The inhibition of nNOS isoform was determined by monitoring the conversion of L-[³H]arginine to L-[³H]citrulline as previously described.⁵²

All the compounds reported here, with the exception of **20** and **21** which were unstable, were tested but none of them showed any significant activity ($\text{IC}_{50} > 100 \mu\text{M}$).

2.3. Refined neural network model

The low-capacity prediction of the model 7 regarding the new derivatives would be due to a lack of data of new compounds during the learning process. Trying to correctly address the model, we decided to refine it. Following the same strategy as for model 7 (strategy 2), we developed model 8 with the 119 inhibitors previously used, plus the seven new synthesized derivatives. This new dataset of compounds was randomly divided in to two sets. According to this distribution, compounds **5**, **6**, **14**, **17** and **18** were included in the training set and compounds **10** and **19** in the test set during model validation. The new model shows acceptable statistical parameters (Tables 2 and 3, entry 8).

Analysis of the classification by category shows that the model 8 correctly evaluates 92.5% for active compounds (1), 50% for moderates, and 93% for inactives (−1) in training sets and 82% for active compounds (1), 40%

for moderates, and 75% for inactives (−1) in test sets.

The results of the training and test sets are gathered in Tables 6 and 7 respectively. This model correctly predicts our compounds according to the experimental data.

3. Conclusions

In summary, we have performed a QSAR study based on different inhibitor families that are able to predict the activity of new compounds. It is interesting to emphasize that CODES is an efficient and easy way to encode structures and it does not need 3D information, thus avoiding the risky choice of the appropriate physicochemical descriptors and problems associated with the conformation.

On the other hand, in relation to the strategies used in the dimension-reduction process, we can conclude that the best results were obtained when the static vector of the four atoms more conserved in all the structures was considered (strategy 2).

Regarding the new-design family, we can conclude that the conformational restriction of the isothiourea group causes a lack of activity, although the synthesized molecules provide nitrogen-containing functional groups as hydrogen-bond donors and alkyl groups for interaction with a hydrophobic site. Probably, the rigidity of the molecules prevents their assuming the appropriate discriminatory-binding orientations.

Table 6. Training set of model 8

| Compound | K_i (μM) | Group ^a | Predicted group |
|----------|-------------------------|--------------------|-----------------|
| I-1 | 0.16 | 1 | 1 |
| I-3 | 0.037 | 1 | 1 |
| I-4 | 0.62 | 1 | 1 |
| I-5 | 0.63 | 1 | 1 |
| I-6 | 14 | -1 | -1 |
| I-7 | 0.8 | 1 | 1 |
| I-11 | 0.25 | 1 | 1 |
| I-12 | 0.016 | 1 | 1 |
| I-13 | 0.1 | 1 | 1 |
| I-14 | 4.8 | 0 | 1 |
| I-15 | 0.12 | 1 | 1 |
| I-16 | 0.25 | 1 | 1 |
| I-18 | 0.45 | 1 | 1 |
| I-20 | 0.17 | 1 | 1 |
| I-21 | 0.56 | 1 | 1 |
| I-22 | 0.29 | 1 | 1 |
| I-23 | 0.7 | 1 | 1 |
| I-24 | 0.19 | 1 | 1 |
| I-25 | 0.21 | 1 | 1 |
| I-26 | 0.34 | 1 | 1 |
| I-29 | 0.18 | 1 | 1 |
| I-30 | 1.1 | 0 | 0 |
| I-33 | 1.4 | 0 | 1 |
| I-34 | 1.1 | 0 | 1 |
| I-35 | 0.32 | 1 | 1 |
| I-37 | 1.4 | 0 | 0 |
| I-40 | 0.8 | 1 | 1 |
| I-44 | 0.68 | 1 | 1 |
| I-45 | 4 | 0 | 1 |
| I-49 | 0.5 | 1 | 1 |
| I-50 | 0.04 | 1 | 0 |
| I-51 | 1.5 | 0 | 0 |
| I-53 | 1 | 1 | 1 |
| I-55 | 0.17 | 1 | 1 |
| I-56 | 2.8 | 0 | 1 |
| I-57 | 2.1 | 0 | 1 |
| I-58 | 0.37 | 1 | 1 |
| I-59 | 0.042 | 1 | 1 |
| I-60 | 0.36 | 1 | 1 |
| I-62 | 1.1 | 0 | 1 |
| I-63 | 0.57 | 1 | 1 |
| I-64 | 1.5 | 0 | 1 |
| I-65 | 0.04 | 1 | 0 |
| I-66 | 0.19 | 1 | 1 |
| I-67 | 0.011 | 1 | 1 |
| I-68 | 0.011 | 1 | 1 |
| I-69 | 0.3 | 1 | 1 |
| I-70 | 0.33 | 1 | 1 |
| I-72 | 0.0087 | 1 | 1 |
| I-73 | 1.7 | 0 | 0 |
| I-74 | 0.1 | 1 | 1 |
| I-77 | 12 | -1 | 0 |
| I-79 | 1.1 | 0 | 0 |
| I-81 | 0.89 | 1 | 1 |
| I-82 | 0.41 | 1 | 0 |
| I-101 | 74 | -1 | -1 |
| I-110 | 14 | -1 | -1 |
| I-111 | 60 | -1 | -1 |
| I-114 | 45 | -1 | -1 |
| I-116 | 12 | -1 | -1 |
| I-117 | 350 | -1 | -1 |
| I-118 | 6 | -1 | -1 |
| I-119 | 2 | 0 | 0 |
| 5 | — | -1 | -1 |
| 6 | — | -1 | -1 |

Table 6 (continued)

| Compound | K_i (μM) | Group ^a | Predicted group |
|----------|-------------------------|--------------------|-----------------|
| 14 | — | -1 | -1 |
| 17 | — | -1 | -1 |
| 18 | — | -1 | -1 |

^a Active (1), moderate (0) or inactive (-1).

Table 7. Test set of model 8

| Compound | K_i (μM) | Group ^a | Predicted group |
|----------|-------------------------|--------------------|-----------------|
| I-2 | 0.029 | 1 | 1 |
| I-8 | 14 | -1 | 1 |
| I-10 | 2 | 0 | 0 |
| I-17 | 0.17 | 1 | 1 |
| I-19 | 0.14 | 1 | 1 |
| I-38 | 4.8 | 0 | 1 |
| I-39 | 1 | 1 | 1 |
| I-41 | 3.3 | 0 | -0 |
| I-43 | 1 | 1 | 1 |
| I-46 | 0.1 | 1 | 1 |
| I-47 | 1.1 | 0 | 1 |
| I-48 | 0.13 | 1 | 1 |
| I-52 | 14 | -1 | 1 |
| I-54 | 0.056 | 1 | 0 |
| I-71 | 0.0063 | 1 | 1 |
| I-78 | 10 | -1 | -1 |
| I-80 | 0.38 | 1 | -1 |
| I-108 | 0.4 | 1 | -1 |
| I-109 | 3 | 0 | -1 |
| I-112 | 50 | -1 | -1 |
| I-113 | 10 | -1 | -1 |
| I-115 | 8 | -1 | -1 |
| 10 | — | -1 | -1 |
| 19 | — | -1 | -1 |

^a Active (1), moderate (0) or inactive (-1).

4. Experimental

4.1. Development of neural models

The following strategy was pursued to develop a neuronal network model to predict nNOS inhibition:

4.1.1. Database. A series of 119 inhibitors were collected from the literature and their biological activity is expressed as K_i (μM) (see Fig. 1 and Table 1). This database is formed by different families, which show K_i values in nNOS. The original database was divided randomly into training sets and test sets of different sizes.

Regarding the output (values of the activity) we used for the training of the neural net: quantitative values to measure the inhibition of $\log K_i$ and qualitative values that refer to assess whether the compounds are active (1), moderate (0) or inactive (-1). Active compounds (1) represent the compounds the activity of which comprises the values until $1 \mu\text{M}$, moderate compounds (0) represent the compounds with activity between 1.1 and $5 \mu\text{M}$ and inactive compounds (-1) represent the compounds with activity higher than $5 \mu\text{M}$.

4.1.2. Input data. The first step is to draw the selected compounds using CHEMDRAW software (v8.0) and encode them using SMILES system (see Table S1 in supporting information) that denotes a molecular structure as a graph.⁵³ This is included in CHEMDRAW software (v8.0). Subsequently, the molecular descriptors are obtained using CODES[®] software (v1.0, revision 3). CODES encodes each molecule into a dynamic matrix. CODES consists of two levels, topological and neural, and its philosophy relies on a Gestalt isomorphism⁵⁴ between both the levels. While the topological space is the chemical structure by itself, the neural one consists of an interactive and competitive network. Each point or atom of the topological space corresponds with each unit or neuron of the neural space, and each type of atom takes a different initial value based on the atom nature, the number of atom bonds, the connectivity with the rest of the molecule, and chirality (if applicable). Attending to connectivity, CODES considers both bonding and not bonding interactions between atoms. If atoms are not bonded in the topological space, it means an inhibitory connection in the neural level (value -1), otherwise the neural space considers an excitatory connection and the value depends on bond type (values: 1 for X–X; 2 for X=X; 3 for X≡X; 1 + 1/2 for aromatic bonds). The stereochemistry is also taken into account during the codification process and *R* or *S* configuration is expressed by a corrective non-linear function.

The neural network employs a sigmoideal function in the codification process and the network is characterized by a non-supervised learning. In the learning process, CODES records all the activities reached in every cycle (or iteration) of the network. This process finishes when the equilibrium state is reached, so, all activity values of each atom of the structure during each cycle or iteration are gathered in a matrix from the initial to the final steps forming the dynamic matrix, which contains the whole codification process.

It is interesting to emphasize that CODES does not need three-dimensional information because the topological space and its conversion to a neural space only need details about points (atoms) and the relationships between them (bonds); that is, the chemical structure by itself. Thus, CODES avoids the risky choice of appropriate physicochemical descriptors and problems associated with the conformation.

Based on the topological matrix, we have developed two different strategies for obtaining the molecular descriptors:

One of these is using the whole previous matrix of each compound. The next step is reduction of dimension of matrices of each chemical in order to have the same number of descriptors or variables.

Reduction of dimension (RD) philosophy resides in reducing the complexity of any system without loss of any intrinsic characteristics or information about the chemical nature. High-dimensional data can be converted to low-dimensional codes by training a supervised multilayer neural network namely ReNDER (Reversible

Non-linear Dimension Reduction). The network consists of five layers of neurons: an input layer, a first hidden layer (coding), a central layer of two or three neurons, a third hidden layer (decoding) and the output layer. The input and output layers contain the same information and therefore the same number of neurons, and the coding and decoding layers are of the same size and the central layer contains a number of neurons equal to the dimensionality of the ReNDER plot required (usually 2 or 3).⁵⁵ In the developed model, the process of dimension-reduction is carried out in order to compress the dynamic matrix data to a set of four numeric codes for each molecule (hidden neurons: A, B, C, and D; see supporting information, Table S1). RD process is carried out using TSAR[®] program⁵⁵ which applies Monte Carlo algorithm. Convergence parameters are 0.005 RMS (Root Mean Square) of convergence, 1000 cycles past best, 3000 iterations/cycle, and data excluding of 1%. The process is finished when Best RMS and Test RMS are constant and their values are not higher than 0.02. If the values were higher, the reductions settings would be 0.0005 RMS of convergence, 4000 cycles past best, 20000 iterations/cycle and 1% of excluded data for testing. The neural network is considered trained when the lines diagrams of the convergence plot are unchanging.

The second one is choice of four parameters per molecule from the last step of the codification process generated by CODES, which correspond to descriptors of the four atoms more conserved in all the structures (Fig. 3). In this way, a static set of four descriptors is obtained (see Supporting information, Table S2).

4.1.3. Development of neural network model. This procedure is carried out by a standard feed-forward network with back-propagation using TSAR software (v3.0)⁵⁵ with an architecture $4 - n - 1$, where four is the parameter above described, n is the hidden neurons, and one is the output value (K_i).

In each training set established, we performed a systematic study of the neural network learning process. In the first approach, we evaluated the suitable number of hidden neurons attending to ρ factor, thus, several initial trainings were carried out with the appropriate architecture. Models were evaluated using statistical parameters and internal validation method (described below) and the best ones were retrained in the second learning stage. We used two different approaches in this second learning phase (see Fig. 2). Via 1 consists in retraining the selected model several times while the second approach, via 2, consists also in several retrainings but in this case, each retraining is used as the previous model in the following one.

4.1.4. Validation of the models. All models were evaluated using some statistical indices: as fraction correct (FC), false alarm rate (FAR), and probability of detection (POD). Before calculating such indices, TA (number of cases that were truly classified as active), TM (number of cases that were truly classified as moderate), TI (number of cases that were truly classified as inactive), FA (number of cases that were wrongly recognized

as active), and FI (number of cases that were wrongly recognized as inactive) should have been counted by each final model.

Fraction correct (FC) is the fraction of compounds that were classified correctly.

$$FC = \frac{TA + TM + TI}{N_{\text{total}}^o} \times 100$$

False alarm rate (FAR) represents the fraction of inactive compounds that were wrongly classified.

$$FAR = \frac{FA}{TA + TM + TI} \times 100$$

Probability of detection (POD) is another index by which we evaluated our models. It represents the fraction of active cases that were truly classified.⁵⁶

$$POD = \frac{TA + TM}{TA + TM + FI} \times 100$$

Moreover, we carried out an internal validation by regression data like s , r , cross-validation expressed by r_{cv}^2 , data that is carried out by leave-group-out method and internal prediction of four randomly excluded structures.

On the other hand, we carried out an external validation by test-set prediction.

4.2. Chemical procedures

Substrates were either purchased from commercial sources or used without further purification. Melting points were determined with a Reichert–Jung Thermovar apparatus and are uncorrected. Flash column chromatography was carried out at medium pressure using silica gel (E. Merck, Grade 60, particle size 0.040–0.063 mm, 230–240 mesh ASTM) with the indicated solvents as eluents. Compounds were detected with UV light (254 nm). ¹H NMR spectra were obtained on Varian INOVA-400, Bruker AVANCE-300, and Varian-Gemini-200 spectrometers working at 400, 300 and 200 MHz, respectively. Typical spectral parameters: spectral width 10 ppm, pulse width 9 μs (57°), and data size 32 K. ¹³C NMR experiments were carried out on the Varian INOVA-400, Bruker AVANCE-300, and Varian-Gemini-200 spectrometers operating at 100, 75, and 50 MHz, respectively. The acquisition parameters: spectral width 16 kHz, acquisition time 0.99 s, pulse width 9 μs (57°), and data size 32 K. Chemical shifts are reported in values (ppm) relative to internal Me₄Si and J values are reported in Hertz. IR (infrared-spectroscopy) was measured on a Perkin-Elmer Spectrum One Spectrometer. EI (electronic ionization mass spectroscopy), MSD 5973 Hewlett Packard and ESI (electrospray ionization mass spectroscopy), and LC/MSD-Serie 100 Hewlett Packard. Elemental analyses were performed by the analytical department at CENQUIOR (CSIC).

4.2.1. 4-Benzyl-2-ethyl-5-methylcarbamoylimino-3-oxo-2,3,4,5-tetrahydro-1,2,4-thiadiazole (10). To a solution of

6⁴³ (0.20 g, 0.90 mmol) in DMF (9.0 mL), triethylamine (0.2 mL, 1.53 mmol) and ethylisocyanate (0.1 mL, 1.42 mmol) were added and the mixture was heated at 80 °C. After 5 h, the reaction mixture was cooled to room temperature and the solvent was removed under reduced pressure. The residue was purified by silica gel column chromatography using dichloromethane/methanol (90:1) as eluent to give a colorless oil. Yield: 0.20 g (79%). Purity >99% (by HPLC). ¹H NMR (200 MHz, CDCl₃): δ 7.43–7.38 (m, 2H, Ar-H), 7.32–7.23 (m, 3H, Ar-H), 5.54–5.52 (br m, 1H, NH), 5.00 (s, 2H, CH₂Ph), 3.58 (c, 2H, J = 7.2 Hz, CH₂), 2.97 (d, 0.3H, J = 5.2 Hz, *anti*-MeNH), 2.85 (d, 2.7H, J = 5.2 Hz, *syn*-MeNH), 1.23 (t, 3H, J = 7.2 Hz, Me). ¹³C NMR (50 MHz, CDCl₃): δ 165.8 (C-5), 165.2 (CONH), 152.5 (C-3), 135.6 (Ar-C), 128.4 (2C, Ar-C), 128.4 (2C, Ar-C), 127.8 (Ar-C), 47.4 (CH₂Ph), 38.9 (CH₂), 27.2 (MeNH), 14.0 (Me). MS (ESI): m/z 293 (M+H)⁺. Anal. Calcd for C₁₃H₁₆N₄O₂S: C, 53.41; H, 5.52; N, 19.16; S, 10.97. Found: C, 53.36; H, 5.73; N, 19.24; S, 10.68.

4.2.2. 4-Benzyl-2-ethyl-5-methylcarbamoylimino-3-thioxo-2,3,4,5-tetrahydro-1,2,4-thiadiazole (11). To a solution of **6⁴³** (0.20 g, 0.90 mmol) in DMF (9.0 mL), triethylamine (0.2 mL, 1.50 mmol) and ethylisothiocyanate (0.1 mL, 1.42 mmol) were added and the mixture was heated at 80 °C. After 15 h, the reaction mixture was cooled to room temperature and the solvent was removed under reduced pressure. The residue was purified by silica gel column chromatography using hexane/ethyl acetate (3:1) as eluent to give a colorless oil. Yield: 0.13 g (46%). Purity >99% (by HPLC). ¹H NMR (400 MHz, DMSO-*d*₆): δ 8.15 (c, 1H, J = 4.8 Hz, NH), 7.38–7.24 (m, 5H, Ph), 5.46 (s, 2H, CH₂Ph), 3.98 (c, 2H, J = 7.2 Hz, CH₂), 2.79 (d, 0.3H, J = 4.8 Hz, *anti*-MeNH), 2.67 (d, 2.7H, J = 4.8 Hz, *syn*-MeNH), 1.24 (t, 3H, J = 7.2 Hz, Me). ¹³C NMR (100 MHz, DMSO-*d*₆): δ 172.1 (C-3), 165.8 (C-5), 164.3 (CONH), 135.4 (Ar-C), 128.3 (2C, Ar-C), 127.4 (2C, Ar-C), 127.3 (Ar-C), 50.7 (CH₂Ph), 43.0 (CH₂), 27.9 (*anti*-MeNH), 26.9 (*syn*-MeNH), 12.9 (Me). MS (ESI): m/z 309 (M+H)⁺. Anal. Calcd for C₁₃H₁₆N₄OS₂: C, 50.63; H, 5.23; N, 18.17; S, 20.79. Found: C, 50.37; H, 5.15; N, 18.26; S, 20.86. IR: ν 3338 (m, NH), 1621 (s, C=O), 1213 (s, C=S) cm⁻¹.

4.2.3. 4-Benzyl-2-(2-methoxy-4-nitrophenyl)-5-methylcarbamoylimino-3-thioxo-2,3,4,5-tetrahydro-1,2,4-thiadiazole (12). To a solution of **6⁴³** (50.0 mg, 0.22 mmol) in DMF (2.2 mL), triethylamine (53.5 μL, 0.38 mmol) and 4-nitro-2-methoxyphenylisothiocyanate (75.0 mg, 0.35 mmol) were added and the mixture was heated at 80 °C. After 48 h, the reaction mixture was cooled to room temperature and the solvent was removed under reduced pressure. The residue was purified by silica gel column chromatography using hexane/ethyl acetate (3:1) as eluent to give a yellow solid. Yield: 25.2 mg (26%). Mp: 180–182 °C. Purity: 97% (by HPLC). ¹H NMR (300 MHz, CDCl₃): δ 7.86 (dd, 1H, J = 8.5, 2.1 Hz, Ar-H), 7.79 (d, 1H, J = 2.1 Hz, Ar-H), 7.52 (dd, 2H, J = 7.3, 2.1 Hz, Ar-H), 7.34–7.32 (br m, 3H, Ar-H), 6.93 (d, 1H, J = 8.5 Hz, Ar-H), 5.56–5.54 (br m, 1H, NH), 5.46 (s, 2H, CH₂Ph), 3.89 (s, 3H, MeO), 3.00 (d, 0.3H, J = 4.9 Hz, *anti*-MeNH), 2.90 (d, 2.7H, J = 4.9 Hz, *syn*-MeNH). ¹³C NMR (75 MHz, CDCl₃): δ 167.9 (C-3), 163.8

(CONH), 156.2 (C-5), 150.8 (NO₂-C), 145.1 (MeO-C), 144.4 (Ar-C), 135.3 (Ar-C), 128.5 (2C, Ar-C), 128.3 (2C, Ar-C), 127.9 (Ar-C), 121.3 (Ar-C), 117.2 (Ar-C), 107.2 (Ar-C), 56.1 (MeO), 51.7 (CH₂Ph), 29.6 (*anti*-MeNH), 27.3 (*syn*-MeNH). MS (ESI): *m/z* 432 (M+H)⁺, 885 (2M+Na)⁺.

4.2.4. 4-Benzyl-2-*tert*-butyl-5-methylcarbamoylimino-3-thioxo-2,3,4,5-tetrahydro-1,2,4-thiadiazole (13). To a solution of **6**⁴³ (50.0 mg, 0.22 mmol) in DMF (2.2 mL), triethylamine (53.5 μ L, 0.38 mmol) and *tert*-butylisothiocyanate (45.2 μ L, 0.35 mmol) were added and the mixture was heated at 80 °C. After 48 h, the reaction mixture was cooled to room temperature and the solvent was removed under reduced pressure. The residue was purified by silica gel column chromatography using hexane/ethyl acetate (3:1) as eluent to give a colorless oil. Yield: 15.0 mg (20%). Purity >99% (by HPLC). ¹H NMR (200 MHz, CDCl₃): δ 7.45 (dd, 2H, *J*=7.4, 2.2 Hz, Ar-H), 7.32–7.25 (m, 3H, Ar-H), 5.57 (s, 2H, CH₂Ph), 5.51–5.49 (br m, 1H, NH), 2.96 (d, 0.3H, *J* = 5.0 Hz, *anti*-MeNH), 2.87 (d, 2.7H, *J* = 5.0 Hz, *syn*-MeNH), 1.81 (s, 9H, Me₃). ¹³C NMR (75 MHz, CDCl₃): δ 172.2 (C-3), 166.0 (C-5), 165.0 (CONH), 135.6 (Ar-C), 128.2 (2C, Ar-C), 128.2 (2C, Ar-C), 127.5 (Ar-C), 50.4 (CH₂Ph), 29.5 (C-^tBu), 28.0 (3C, Me₃), 27.4 (MeNH). MS (EI): *m/z* 336 (M⁺, 30).

4.2.5. 5-Benzoylimino-4-cyanomethyl-3-oxo-2,3,4,5-tetrahydro-1,2,4-thiadiazole (14). To a solution of **4**⁴³ (0.15 g, 0.67 mmol) in anhydrous DMF (6.7 mL), K₂CO₃ (58.1 mg, 0.42 mmol) was added and the mixture was stirred at room temperature. After 1 h, chloroacetonitrile (26.5 μ L, 0.42 mmol) was added and the reaction mixture was heated at 60 °C. After 63 h, the reaction mixture was cooled to room temperature and cold distilled water (10.0 mL) was added. The resulting precipitate was isolated by filtration and the solid was purified by silica gel column chromatography using hexane/ethyl acetate (3:2) as eluent to give the monoalkylated product as a white solid. Yield: 0.10 g (60%). Mp: 129–131 °C. ¹H NMR (300 MHz, DMSO-*d*₆): δ 8.22 (d, 2H, *J* = 7.1 Hz, Ar-H), 7.62–7.49 (m, 3H, Ar-H), 4.99 (s, 2H, CH₂), 3.50 (br s, 1H, NH). ¹³C NMR (75 MHz, DMSO-*d*₆): δ 175.3 (PhCO), 173.5 (C-5), 154.3 (C-3), 135.0 (Ar-C), 132.4 (Ar-C), 129.1 (2C, Ar-C), 128.5 (2C, Ar-C), 115.6 (CN), 31.3 (CH₂). MS (EI): *m/z* 260 (M⁺, 9). Anal. Calcd for C₁₁H₈N₄O₂S: C, 50.76; H, 3.10; N, 21.53; S, 12.32. Found: C, 50.39; H, 3.17; N, 21.28; S, 12.47.

4.2.6. 5-Benzoylimino-2,4-bis(cyanomethyl)-3-oxo-2,3,4,5-tetrahydro-1,2,4-thiadiazole (15). To a solution of **4**⁴³ (0.15 g, 0.67 mmol) in anhydrous DMF (6.7 mL), K₂CO₃ (58.1 mg, 0.42 mmol) was added and the mixture was stirred at room temperature. After 1 h, chloroacetonitrile (26.5 μ L, 0.42 mmol) was added and the reaction mixture was heated at 80 °C. After 22 h, the reaction mixture was cooled to room temperature and cold distilled water (10.0 mL) was added. The resulting precipitate was isolated by filtration and the solid was purified by silica gel column chromatography using hexane/ethyl acetate (3:2) as eluent to give the dialkylated product as a white solid. Yield: 0.15 g (75%). Mp: 150–152 °C. ¹H

NMR (300 MHz, DMSO-*d*₆): δ 8.28 (d, 2H, *J* = 7.1 Hz, Ar-H), 7.72 (t, 1H, *J* = 7.3 Hz, Ar-H), 7.61 (dd, 2H, *J* = 7.3, 7.1 Hz, Ar-H), 5.19 (s, 2H, CH₂-4), 4.89 (s, 2H, CH₂-2). ¹³C NMR (75 MHz, DMSO-*d*₆): δ 178.1 (PhCO), 169.4 (C-5), 150.8 (C-3), 134.0 (Ar-C), 132.2 (Ar-C), 129.5 (2C, Ar-C), 129.0 (2C, Ar-C), 115.6 (CN-2), 114.5 (CN-4), 32.2 (CH₂-4), 31.5 (CH₂-2). MS (EI): *m/z* 299 (M⁺, 8). Anal. Calcd for C₁₃H₉N₅O₂S: C, 52.17; H, 3.03; N, 23.40; S, 10.71. Found: C, 52.23; H, 3.17; N, 23.76; S, 10.50.

4.2.7. 5-Benzoylimino-4-cyanomethyl-2-methyl-3-oxo-2,3,4,5-tetrahydro-1,2,4-thiadiazole (16). To a solution of **5**⁴³ (0.15 g, 0.63 mmol) in anhydrous DMF (6.3 mL), K₂CO₃ (54.6 mg, 0.39 mmol) was added and the mixture was stirred at room temperature. After 1 h, chloroacetonitrile (24.9 μ L, 0.39 mmol) was added and the reaction mixture was heated at 80 °C. After 2.5 h, the reaction mixture was cooled to room temperature and cold distilled water (10.0 mL) was added. The resulting precipitate was isolated by filtration to give a white solid. Yield: 0.17 g (97%). Mp: 219–221 °C. ¹H NMR (300 MHz, DMSO-*d*₆): δ 8.27 (d, 2H, *J* = 7.1 Hz, Ar-H), 7.69 (t, 1H, *J* = 7.3 Hz, Ar-H), 7.59 (dd, 2H, *J* = 7.3, 7.1 Hz, Ar-H), 5.16 (s, 2H, CH₂), 3.17 (s, 3H, Me). ¹³C NMR (75 MHz, DMSO-*d*₆): δ 177.4 (PhCO), 168.7 (C-5), 150.8 (C-3), 133.7 (Ar-C), 132.8 (Ar-C), 129.4 (2C, Ar-C), 128.9 (2C, Ar-C), 114.8 (CN), 32.1 (CH₂), 30.2 (Me). MS (EI): *m/z* 274 (M⁺, 14). Anal. Calcd for C₁₂H₁₀N₄O₂S: C, 52.54; H, 3.67; N, 20.43; S, 11.69. Found: C, 52.31; H, 3.74; N, 20.64; S, 11.88.

4.2.8. 4-Aminocarbohydroxymoylmethyl-5-benzoylimino-2-methyl-3-oxo-2,3,4,5-tetrahydro-1,2,4-thiadiazole (17). To a suspension of hydroxylamine hydrochloride (0.12 g, 1.82 mmol) in DMSO (2.0 mL), triethylamine (0.2 mL, 1.82 mmol) was added and the resulting salts were filtered off and washed with THF. The filtrate was concentrated in vacuo to remove THF and **16** (0.10 g, 0.36 mmol) was added to the DMSO solution of hydroxylamine. The reaction mixture was stirred at 75 °C for 8 h and distilled water (4.0 mL) was added. The resulting precipitate was isolated by filtration to give a white solid. Yield: 95.7 mg (85%). Mp: 244–246 °C. ¹H NMR (300 MHz, DMSO-*d*₆): δ 9.23 (s, 1H, OH), 8.18 (dd, 2H, *J* = 7.1, 1.4 Hz, Ar-H), 7.65 (t, 1H, *J* = 7.4 Hz, Ar-H), 7.55 (dd, 2H, *J* = 7.4, 7.1 Hz, Ar-H), 5.63 (br s, 2H, NH₂), 4.65 (s, 2H, CH₂), 3.15 (s, 3H, Me). ¹³C NMR (75 MHz, DMSO-*d*₆): δ 177.3 (PhCO), 169.6 (C-5), 151.9 (C-3), 146.7 (C=NOH), 133.3 (Ar-C), 133.2 (Ar-C), 129.2 (2C, Ar-C), 128.8 (2C, Ar-C), 43.6 (CH₂), 29.8 (Me). MS (ESI): *m/z* 308 (M+H)⁺, 637 (2M+Na)⁺. Anal. Calcd for C₁₂H₁₃N₅O₃S: C, 46.90; H, 4.26; N, 22.79; S, 10.43. Found: C, 47.03; H, 3.99; N, 22.58; S, 10.78.

4.2.9. 5-Benzoylimino-4-methoxycarbonimidoylmethyl-2-methyl-3-oxo-2,3,4,5-tetrahydro-1,2,4-thiadiazole (18) and 5-benzoylimino-4-hydroxycarbonimidoylmethyl-2-methyl-3-oxo-2,3,4,5-tetrahydro-1,2,4-thiadiazole (19). To a solution of **16** (75.0 mg, 0.27 mmol) in MeOH (2.7 mL), MeONa was added (1.4 mg, 0.02 mmol) and

the mixture was stirred at room temperature. After 4 h, the product **18** was obtained as a precipitate, being isolated by filtration to give a white solid. Sometimes, traces of the hydrolysis by-product, **19**, were identified. Then, the purification employing silica gel column chromatography with ethyl acetate/hexane (2:1) as eluent, produced the hydrolysis of **18** into **19** and allowed the isolation of compound **19** as a white solid. First fraction, yield of compound **18**, 77.0 mg (92%). Mp: 182–184 °C. Purity >99% (by HPLC). ¹H NMR (300 MHz, CDCl₃): δ 8.22 (d, 2H, *J* = 7.1 Hz, Ar-H), 7.56 (t, 1H, *J* = 7.3 Hz, Ar-H), 7.46 (dd, 2H, *J* = 7.3, 7.1 Hz, Ar-H), 7.32 (br s, 1H, NH), 4.78 (s, 2H, CH₂), 3.80 (s, 3H, OMe), 3.22 (s, 3H, Me). ¹³C NMR (75 MHz, CDCl₃): δ 178.6 (PhCO), 169.2 (C-5), 165.8 (C=NH), 151.8 (C-3), 133.3 (Ar-C), 133.0 (Ar-C), 129.7 (2C, Ar-C), 128.4 (2C, Ar-C), 53.8 (OMe), 46.1 (CH₂), 30.0 (Me). MS (ESI): *m/z* 307 (M+H)⁺, 329 (M+Na)⁺, 635 (2M+Na)⁺. Anal. Calcd for C₁₃H₁₄N₄O₃S: C, 50.97; H, 4.61; N, 18.29; S, 10.47. Found: C, 50.69; H, 4.48; N, 18.07; S, 10.75. Second fraction, yield compound **19**, Mp: 277–279 °C. Purity >99% (by HPLC). ¹H NMR (300 MHz, DMSO-*d*₆): δ 8.17 (dd, 2H, *J* = 7.1, 1.3 Hz, Ar-H), 7.81 (br s, 1H, OH), 7.65 (t, 1H, *J* = 7.3 Hz, Ar-H), 7.54 (dd, 2H, *J* = 7.3, 7.1 Hz, Ar-H), 7.35 (br s, 1H, NH), 4.60 (s, 2H, CH₂), 3.17 (s, 3H, Me). ¹³C NMR (75 MHz, DMSO-*d*₆): δ 177.2 (PhCO), 169.5 (C-5), 167.1 (C=NH), 152.0 (C-3), 133.4 (Ar-C), 133.1 (Ar-C), 129.2 (2C, Ar-C), 128.8 (2C, Ar-C), 46.4 (CH₂), 29.9 (Me). MS (ESI): *m/z* 293 (M+H)⁺, 315 (M + Na)⁺, 607 (2M+Na)⁺.

4.2.10. 5-Benzoylimino-2-methyl-3-oxo-4-(N¹-phenylamidinomethyl)-2,3,4,5-tetrahydro-1,2,4-thiadiazole hydrochloride (20). To a solution of **18** (50.0 mg, 0.16 mmol) in MeOH (1.6 mL), distilled aniline (15.0 μL, 0.17 mmol) was added and the mixture was stirred at 40 °C. After 32 h, the reaction mixture was cooled to room temperature, saturated with dry hydrogen chloride gas and stirred for a few minutes to remove the excess of hydrogen chloride gas. The solvent was evaporated under reduced pressure and dichloromethane was added to the residue. The resulting precipitate was isolated by filtration to give a white solid. Yield: 4.0 mg (6%). ¹H NMR (400 MHz, DMSO-*d*₆): δ 11.73 (br s, 1H, PhNH), 9.77 (br s, 1H, C=NH₂Cl), 8.97 (br s, 1H, C=NH₂Cl), 8.20 (d, 2H, *J* = 7.2 Hz, Ar-H), 7.66 (t, 1H, *J* = 7.4 Hz, Ar-H), 7.57–7.50 (m, 4H, Ar-H), 7.41 (t, 1H, *J* = 7.2 Hz, Ar-H), 7.27 (d, 2H, *J* = 7.6 Hz, Ar-H), 5.18 (s, 2H, CH₂), 3.19 (s, 3H, Me). MS (EI): *m/z* 367 (M⁺–HCl, 12).

4.2.11. 5-Benzoylimino-4-hydrazinocarbonimidoylmethyl-2-methyl-3-oxo-2,3,4,5-tetrahydro-1,2,4-thiadiazole (21). To a solution of **16** (50.0 mg, 0.18 mmol) in MeOH (1.8 mL), MeONa (9.8 mg, 0.18 mmol) was added and the mixture was stirred for 2 h until the imido ester **18** was obtained. Hydrazine Hydrochloride (13.7 mg, 0.20 mmol) was added to the reaction mixture and stirred at 45 °C. After 72 h, the reaction mixture was cooled to room temperature and the resulting precipitate was filtered to give a white solid. Yield: 27.0 mg (48%). ¹H NMR (200 MHz, DMSO-*d*₆): δ 8.36 (br s, 1H, NH), 8.12 (br m, 2H, Ar-H), 7.64–7.49 (m, 3H, Ar-H), 6.27

(br s, 1H, C=NH), 5.75 (s, 2H, CH₂), 5.40 (br s, 1H, NH₂), 4.59 (br s, 1H, NH₂), 3.15 (s, 3H, Me). ¹³C NMR (75 MHz, CDCl₃): δ 177.4 (PhCO), 169.5 (C-5), 150.2 (C-3), 149.7 (C=NH), 133.4 (Ar-C), 133.0 (Ar-C), 129.2 (2C, Ar-C), 128.7 (2C, Ar-C), 55.1 (CH₂), 30.1 (Me). MS (EI): *m/z* 306 (M⁺, 1).

Acknowledgments

We gratefully acknowledge the financial support, for this project, of CICYT (SAF2006/01249). Thanks are also due to Dr. Juan Antonio Pérez for his helpful discussions on the manuscript. Tania Castaño and Arantxa Encinas acknowledge a predoctoral fellowship from the Spanish Ministry of Education and Science.

Supplementary data

Supplementary data associated with this article can be found, in the online version, at doi:10.1016/j.bmc.2008.04.036.

References and notes

- Kapoor, R. *Curr. Opin. Neurol.* **2006**, *19*, 255–259.
- Poewe, W. *Neurology* **2006**, *66*, S2–S9.
- Thatcher, G. R.; Bennett, B. M.; Reynolds, J. N. *Curr. Alzheimer Res.* **2006**, *3*, 237–245.
- Casetta, I.; Govoni, V.; Granieri, E. *Curr. Pharm. Des.* **2005**, *11*, 2033–2052.
- Zhu, X.; Raina, A. K.; Perry, G.; Smith, M. A. *Lancet Neurol.* **2004**, *3*, 219–226.
- Nunomura, A.; Perry, G.; Aliev, G.; Hirai, K.; Takeda, A.; Balraj, E. K.; Jones, P. K.; Ghanbari, H.; Wataya, T.; Shimohama, S.; Chiba, S.; Atwood, C. S.; Petersen, R. B.; Smith, M. A. *J. Neuropathol. Exp. Neurol.* **2001**, *60*, 759–767.
- Nunomura, A.; Perry, G.; Pappolla, M. A.; Friedland, R. P.; Hirai, K.; Chiba, S.; Smith, M. A. *J. Neuropathol. Exp. Neurol.* **2000**, *59*, 1011–1017.
- Moreira, P. I.; Honda, K.; Liu, Q.; Santos, M. S.; Oliveira, C. R.; Aliev, G.; Nunomura, A.; Zhu, X.; Smith, M. A.; Perry, G. *Curr. Alzheimer Res.* **2005**, *2*, 403–408.
- Heneka, M. T.; Feinstein, D. L. *J. Neuroimmunol.* **2001**, *114*, 8–18.
- Alderton, W. K.; Cooper, C. E.; Knowles, R. G. *Biochem. J.* **2001**, *357*, 593–615.
- Low, S. Y. *Mol. Aspects Med.* **2005**, *26*, 97–138.
- Salerno, L.; Sorrenti, V.; Di Giacomo, C.; Romeo, G.; Siracusa, M. A. *Curr. Pharm. Des.* **2002**, *8*, 177–200.
- Fan, J.-S.; Zhang, Q.; Li, M.; Tochio, H.; Yamazaki, T.; Shimizu, M.; Zhang, M. *J. Biol. Chem.* **1998**, *273*, 33472–33481.
- Schulz, J. B.; Matthews, R. T.; Klockgether, T.; Dichgans, J.; Flint Beal, M. *Mol. Cell. Biochem.* **1997**, *174*, 193–197.
- Macdonald, J. E. *Ann. Rep. Med. Chem.* **1996**, 221–230.
- Babu, B. R.; Griffith, O. W. *Curr. Opin. Chem. Biol.* **1998**, *2*, 491–500.
- Garvey, E. P.; Oplinger, J. A.; Tanoury, G. J.; Sherman, P. A.; Fowler, M.; Marshall, S.; Harmon, M. F.; Paith, J. E.; Furfine, E. S. *J. Biol. Chem.* **1994**, *269*, 26669–26676.
- Shearer, B. G.; Lee, S. L.; Oplinger, J. A.; Frick, L. W.; Garvey, E. P.; Furfine, E. S. *J. Med. Chem.* **1997**, *40*, 1901–1905.
- Wolff, D. J.; Gauld, D. S.; Neulander, M. J.; Southan, G. *J. Pharmacol. Exp. Ther.* **1997**, *283*, 265–273.

20. Ruetten, H.; Southan, G. J.; Abate, A.; Thiemermann, C. *Br. J. Pharmacol.* **1996**, *118*, 261–270.
21. Gomez-Vidal, J. A.; Martásek, P.; Roman, L. J.; Silverman, R. B. *J. Med. Chem.* **2004**, *47*, 703–710.
22. Furfine, E. S.; Harmon, M. F.; Paith, J. E.; Garvey, E. P. *Biochemistry* **1993**, *32*, 8512–8517.
23. Di Giacomo, C.; Sorrenti, V.; Salerno, L.; Cardile, V.; Guerrera, F.; Siracusa, M. A.; Avitabile, M.; Vanella, A. *Exp. Biol. Med.* **2003**, *228*, 486–490.
24. Hagen, T. J.; Bergmanis, A. A.; Kramer, S. W.; Fok, K. F.; Schmelzer, A. E.; Pitzele, B. S.; Swenton, L.; Jerome, G. M.; Kornmeier, C. M.; Moore, W. M.; Branson, L. F.; Connor, J. R.; Manning, P. T.; Currie, M. G.; Hallinan, E. A. *J. Med. Chem.* **1998**, *41*, 3675–3683.
25. Collins, J. L.; Shearer, B. G.; Oplinger, J. A.; Lee, S. L.; Garvey, E. P.; Salter, M.; Duffy, C.; Burnette, T. C.; Furfine, E. S. *J. Med. Chem.* **1998**, *41*, 2858–2871.
26. Babu, B. R.; Griffith, O. W. *J. Biol. Chem.* **1998**, *273*, 8882–8889.
27. Lee, Y.; Martasek, P.; Roman, L. J.; Masters, B. S.; Silverman, R. B. *Bioorg. Med. Chem.* **1999**, *7*, 1941–1951.
28. Sorrenti, V.; Di Giacomo, C.; Salerno, L.; Siracusa, M. A.; Guerrera, F.; Vanella, A. *Nitric oxide* **2001**, *5*, 32–38.
29. Salerno, L.; Sorrenti, V.; Guerrera, F.; Sarva, M. C.; Siracusa, M. A.; Di Giacomo, C.; Vanella, A. *Pharmazie* **1999**, *54*, 685–690.
30. Lee, Y.; Martasek, P.; Roman, L. J.; Silverman, R. B. *Bioorg. Med. Chem. Lett.* **2000**, *10*, 2771–2774.
31. Lisboa, P. J.; Taktak, A. F. *Neural Netw.* **2006**, *19*, 408–415.
32. Durisova, M.; Dedik, L. *Basic Clin. Pharmacol. Toxicol.* **2005**, *96*, 335–342.
33. Winkler, D. A. *Mol. Biotechnol.* **2004**, *27*, 139–168.
34. Kovesdi, I.; Dominguez-Rodriguez, M. F.; Orfi, L.; Naray-Szabo, G.; Varro, A.; Papp, J. G.; Matyus, P. *Med. Res. Rev.* **1999**, *19*, 249–269.
35. Csermely, P.; Agoston, V.; Pongor, S. *Trends Pharmacol. Sci.* **2005**, *26*, 178–182.
36. Stud, M. CODES® v1.0 (revisión 3).
37. Ochoa, C.; Rodríguez, J.; Rodríguez, M.; Chana, A.; Stud, M.; Alonso-Villalobos, P.; Martínez-Grueiro, M. *Med. Chem. Res.* **1998**, *7*, 530–545.
38. Martínez, A.; Castro, A.; Stud, M.; Rodríguez, J.; Cardelús, I.; Llenas, J.; Fernández, A.; Palacios, J. M. *Med. Chem. Res.* **1998**, *8*, 171–180.
39. Dorronsoro, I.; Chana, A.; Abasolo, I.; Castro, A.; Gil, C.; Stud, M. *QSAR Comb. Sci.* **2004**, *23*, 89–98.
40. Quiñones, C.; Cáceres, J.; Stud, M.; Martínez, A. *Quant. Struct. Act. Relat.* **2000**, *19*, 448–454.
41. Narayanan, K.; Griffith, O. W. *J. Med. Chem.* **1994**, *37*, 885–887.
42. Li, H. Y.; Raman, C. S.; Martasek, P.; Kral, V.; Masters, B. S. S.; Poulos, T. L. *J. Inorg. Biochem.* **2000**, *81*, 133–139.
43. Castro, A.; Encinas, A.; Gil, C.; Brase, S.; Porcal, W.; Perez, C.; Moreno, F. J.; Martínez, A. *Bioorg. Med. Chem.* **2008**, *16*, 495–510.
44. Singh, R.; Choubey, K.; Bhattacharya, A. *J. Indian Chem. Soc.* **1998**, *75*, 430–431.
45. Yuan, H. L.; Cho, N. S.; Jaw, J.-H. J.; Woodhouse, T. E.; Aung, T. L. *J. Het. Chem.* **1989**, *26*, 1331–1334.
46. Cho, N. S.; Shon, H. I.; Párkányi, C. *J. Het. Chem.* **1991**, *28*, 1645–1649.
47. L'abbé, G.; Albrecht, E. *J. Het. Chem.* **1992**, *29*, 451–454.
48. Guard, J. A. M.; Steel, P. J. *Aust. J. Chem.* **1995**, *48*, 1609–1615.
49. Kohara, Y.; Kubo, K.; Imamiya, E.; Wada, T.; Inada, Y.; Naka, T. *J. Med. Chem.* **1996**, *39*, 5228–5235.
50. Pinner, A. *Die Imidoäther und ihre Derivate*; Oppenheim: Berlin, 1892.
51. Bolhofer, W. A.; Habecker, C. N.; Pietruszkiewicz, A. M.; Torchiana, M. L.; Jacoby, H. I.; Stone, C. A. *J. Med. Chem.* **1979**, *22*, 295–301.
52. Bredt, D. S.; Snyder, S. H. *Proc. Natl. Acad. Sci. U.S.A.* **1989**, *86*, 9030–9033.
53. Weininger, D. *J. Chem. Inf. Comput. Sci.* **1988**, *28*, 31–36.
54. Kohler, W. *The Task of Gestalt Psychology*; Princeton University Press (Princeton): New Jersey, 1969.
55. TSAR® v3.3. Oxford Molecular Ltd.
56. Sadat Hayatshahi, S. H.; Abdolmaleki, P.; Safarian, S.; Khajeh, K. *Biochem. Biophys. Res. Commun.* **2005**, *338*, 1137–1142.